Project funded by the European Commission under the 6th (EC) RTD Framework Programme (2002- 2006) within the framework of the specific research and technological development programme “Integrating and strengthening the European Research Area”

Project UpWind.TTC

Contract No.:
019945 (SES6)

“Integrated Wind Turbine Design”

Micromechanical fatigue strength theory of composite

AUTHOR:	Dr Volodymyr Kushch
AFFILIATION:	Institute for Superhard Materials NAS of Ukraine
ADDRESS:	2 Avtozavodskaya Str., 04074 Kyiv Ukraine
TEL.:	+38 044 432 9544
EMAIL:	vkushch@bigmir.net
FURTHER AUTHORS:	Sergiy V. Shmegera, Yaroslav O. Podoba, Dr Leon Mishnaevsky Jr
REVIEWER:	Project members
APPROVER:	

Document Information

DOCUMENT TYPE	Deliverable
DOCUMENT NAME:	Micromechanical fatigue strength theory of composite
REVISION:	
REV.DATE:	
CLASSIFICATION:	R1: Restricted to project members
STATUS:	complete

Abstract: The micromechanical fatigue strength theory of fibrous composites has been developed, with a special attention to the interface damage onset and accumulation. The method combines the multipole expansion technique with the representative unit cell model of random structure composite. Both experimental observations and numerical simulation show a clear tendency of the interface cracks to form the chain-like clusters, oriented predominantly across the loading direction. Clustering of interface cracks, in turn, accelerates the stiffness loss in the direction of loading and increases the damage-induced elastic anisotropy of the effective elastic moduli of composite. This is especially true for the high-filled FRCs widely used in the engineering practice. It is obvious that a single fiber approximation does not work here and one has to look for the multiple fiber models. Among them, the multiple fiber representative unit cell model is, probably, the best choice as it provides a comprehensive account of microstructure and interactions between the fibers which cannot be expected in the mean field or Eshelby-type models. The developed theory captures the essential physical nature of the fatigue process and thus provides a reliable theoretical framework for a deeper insight into the damage initiation and accumulation phenomena in the fiber reinforced composites.

Contents

STATUS, CONFIDENTIALITY AND ACCESSIBILITY										
Status				**Confidentiality**				**Accessibility**		
S0	Approved/Released			**R0**	General public			Private web site		
S1	Reviewed			**R1**	Restricted to project members	**R1**		Public web site		
S2	Pending for review			**R2**	Restricted to European. Commission			Paper copy		
S3	Draft for commends			**R3**	Restricted to WP members + PL					
S4	Under preparation			**R4**	Restricted to Task members +WPL+PL					

PL: *Project leader* **WPL:** *Work package leader* **TL:** *Task leader*

1 Interface damage models: an overview

Mechanical behavior of composite materials is significantly affected by the degree of bonding between the constituents. Interfacial debonding in the form of arc crack is the predominant damage mode of unidirectional fiber reinforced composite (FRC) under transverse loading, resulting in rapid loss of stiffness and strength. From the viewpoint of damage-tolerant design of composite structures, it is important to provide optimal balance between strength and stiffness. To achieve this goal, an effect of interface debonding on the performance of composite needs to be fully understood and adequately implemented in the predictive models.

An effect of weak bond or debonded interface on the mechanical properties has been studied by several investigators. Benveniste (1985) simulated the imperfect interface by imposing the continuity of normal displacements and tractions at the interface while allowing a jump in the tangential displacement. Hashin (1990) assumed the linear relationship between interface tractions and displacement jumps and used the self-consistent scheme to predict the effective moduli of the composite. In the work by Lee and Simunovic(2001), the partially debonded fibers are regarded as equivalent, transversely isotropic inclusions. Only a few publications are available where the models explicitly involving the interface cracks are considered. Toya (1974) has obtained the Eshelby-type solution for a single, partially debonded circular inclusion. The known analytical solutions for the non-uniform far stress field are confined to the works by Prasad and Simha (2003) and Theotokoglou and Theotokoglou (2002) where the concentrated force and dislocation applied at the point in the matrix containing a single partially debonded circular inclusion were considered.

There is a number of publications on stiffness prediction for fibrous composites with interfacial debonding by means of micromechanics. However, the most existing work is based on models of varying degrees of approximation in the treatment of fiber interaction and local stress and strain fields. Among them, the "dilute" composite model (Ju, 1991; Lee and Simunovic, 2001) where the effect of fiber interaction is neglected. In the self-consistent "composite cylinder" models used by Teng (1992) and Tandon and Pagano (1996), interaction between fibers is taken into account in approximate manner. In these works, the debonding configuration consists of two symmetrically located interface cracks. The Mori-Tanaka method-based model by Takahashi and Chou (1988) assumes debonding to take place over the entire interface. A dual effective-medium and finite-element study was carried out by Zheng et al. (2000) and Zhao and Weng (2002) for a composite containing partially debonded elliptic fiber. In the effective-medium approach, the fictitious perfectly bonded inclusions were used and the Mori-Tanaka theory was applied to compute the effective moduli of composite.

In the more advanced, representative unit cell (RUC) approach, an actual FRC is modeled by the equivalent (in some sense) periodic micro structure with a cell containing a certain number of inclusions. This model is advantageous in that enables taking into account interactions among a whole infinite array of inhomogeneities whereas the deterministic geometry enables an accurate solution of the model problem. These features make the RUC approach appropriate for studying the high-filled strongly heterogeneous composites, where the structure and interactions between the fibers should be taken into account accurately.

In application to the considered problem, the simplest model of this kind is the composite with a regular (square of hexagonal) arrangement of equally debonded fibers. In this case, the composite stiffness can be determined by analyzing a unit cell containing a single fiber.

In the elastic contact model by Shan and Chou (1995), the fiber-matrix interface is assumed completely debonded. Yuan et al. (1997) simulated the debonded interface is by uni-symmetric and doubly-symmetric interface cracks. In these papers, the interface bonding conditions are fixed in the problem statement. The interfacial failure option was implemented by Yeh (1992) and Aghdam et al. (2008) by means of interface/interphase elements and by Caporale et al. (2006) who modeled interfacial failure by the brittle-elastic springs.

The drawback of single fiber cell model consists in that it implies all the fibers to be equally loaded/debonded. In fact, damage of FRC is a progressive and cumulative process governed predominantly by the micro structure of composite and elastic interactions between the fibers. These factors cannot be adequately captured by the simple geometry models. Reliable prediction of damage onset/accumulation and resulting evolutionary change of stiffness and strength requires (a) the quasi-random geometry model statistically close to the micro structure of specific FRC; (b) accurate evaluation of the local stress concentrations and (c) application of the adequate interface damage/separation model.

To date, only a few models for the multiple fibers with imperfect interface are available in literature. Wriggers at al (1998) considered debonding by a contact formulation which can handle adhesional forces up to a prescribed tensile limit on the contact interface. In the work by Ghosh et al (2000), interfacial debonding is accommodated by cohesive zone model, in which normal and tangential springs tractions are expressed in terms of interfacial separation. The model by Teng (2007) contains a periodic square array of fibers, with a random subset of them assigned to be completely debonded. The model problem is solved numerically under assumption of frictionless contact at the debonded interfaces and the effective stiffness of composite is found by the ensemble averaging. Recently, a complete analytical solution has been derived by Kushch et al. (2010) for a finite array of interacting, partially debonded circular inclusions. The developed method combines the superposition principle with the complex potentials technique and results in a simple and highly efficient numerical algorithm. The method provides an accurate analysis of the local fields, stress intensity factors and the energy release rate at the interface crack tips which are greatly affected by elastic interaction between the partially debonded inclusions.

In the present work, we extend the approach by Kushch et al. (2010) on the RUC model of fibrous composite with interface cracks. The multiple fiber cell geometry is chosen so that it provides seamless joint with the adjacent cells. A complete analytical solution in displacements has been obtained in terms of the periodic complex potentials. By analytical averaging the local strain and stress fields, the exact expressions of the effective transverse elastic moduli have been found. Several test problems have been solved to check an accuracy and numerical efficiency of the method. Numerical simulation of interface damage accumulation and clustering in FRC has been performed and the caused by it stiffness reduction is estimated.

2 Thermodynamic definition of macro damage tensor

The modern continuuum theories used in design of composite structures employ a fourth-rank macroscopic damage tensor to represent the state of damage in composite materials. It is worth mentioning that the fourth-rank damage tensor has an appealing correspondence with the fourth-rank overall compliance tensor. Within the framework of homogenization concept

for inhomogeneous effective continuum medium, one may define the homogenized Gibbs free energy as (Ju, 1991)

$$\chi \equiv \frac{1}{2}\mathbf{S} : [\mathbf{L}_0^* \cdot (\mathbf{I} + \mathbf{D})] : \mathbf{S} \tag{1}$$

where $\mathbf{S}$ is the volume-average stress tensor, $\mathbf{L}_0^* = (\mathbf{C}_0^*)^{-1}$ is the effective compliance and $\mathbf{C}_0^*$ is the effective stiffness of the undamaged composite material, $\mathbf{I}$ is the fourth-rank unit tensor, $\mathbf{D}$ denotes the fourthrank damage tensor, and " : " denotes the tensor contraction operation. It is emphasized that $\mathbf{D}$ is an evolving tensorial state variable, not a constant tensor: see Ju (1991) for more thermodynamics details.

By the Clausius-Duhem inequality for isothermal process, we have ($\mathbf{E}$ is the volume-average strain)

$$\dot{\chi} - \dot{\mathbf{S}} : \mathbf{E} \geq 0. \tag{2}$$

The standard Coleman's method then leads to the following macroscopic stress-strain law and overall elastic-damage compliance tensor S:

$$\mathbf{E} = \mathbf{L}^* : \mathbf{S}; \qquad \mathbf{L}^* = [\mathbf{L}_0^* \cdot (\mathbf{I} + \mathbf{D})] \tag{3}$$

together with the damage dissipative inequality:

$$\frac{1}{2}\mathbf{S} : \dot{\mathbf{L}^*} : \mathbf{S} > 0, \quad \text{or} \quad \frac{1}{2}\mathbf{S} : [\mathbf{L}_0^* \cdot \dot{\mathbf{D}}] : \mathbf{S} > 0. \tag{4}$$

From (4) it is observed that the evolution $\dot{\mathbf{L}^*}$ (or $\dot{\mathbf{D}}$) plays an essential role in microcrack energy dissipation and growth.

During a damage loading process, the total strain tensor e is amenable to an additive decomposition: $\mathbf{E} = \mathbf{E}_e + \mathbf{E}_d$, where $\mathbf{E}_e$ and $\mathbf{E}_d$ denote the elastic and damage-induced strains, respectively. The elastic-damage compliance tensor is also suitable for an additive decomposition: $\mathbf{L}^* = \mathbf{L}_0^* + \mathbf{L}_d^*$, where $\mathbf{L}_d^*$ signifies the damage-induced compliance. Clearly, the relationship between $\mathbf{L}_d^*$ and $\mathbf{D}$ can be formally expressed as $\mathbf{L}_d^* = \mathbf{L}_0^* - \mathbf{D}$. Therefore, if one can derive the damage induced compliance $\mathbf{L}_d^*$ from the "first principles", then one can explicitly express the fourth-rank damage tensor $\mathbf{D}$ by means of micromechanics. The developed below model of FRC with interface damage provides a reliable basis for the *micromechanical* theories of static and fatigue strength of fibrous composites.

3 Micromechenical model of FRC

3.1 Geometry

We consider a quasi-random model of the FRC bulk (Golovchan et al., 1993; Bystroem, 2003; Chen and Papathanasiou, 2004; Kushch et al, 2008; among others) with the period a along the axes Ox_1 and Ox_2, The representative unit cell (RUC) of it containing the centres of N_p of aligned in x_3-direction and circular in cross-section fibers is shown in Fig.1. Within a cell, the fibers can be placed arbitrarily but without overlapping. Alternatively, this model can be thought as an infinite plane containing N_p non-overlapping periodic square arrays of fibers.

The fibers shown by the dashed line do not belong to the cell while occupying a certain area within it. The fiber volume content is $c = N_p\pi/a^2$.

Thus, geometry of the unit cell is given by its side length a and the coordinates (X_{1q}, X_{2q}) defining the center of qth fiber, $q = 1, 2, ..., N_p$. Number N_p can be taken large sufficiently to simulate micro structure of an actual disordered composite. To reduce a number of parameters and to simplify the notations, we assume the fibers equally sized, of radius $R = 1$, and made from the same material.

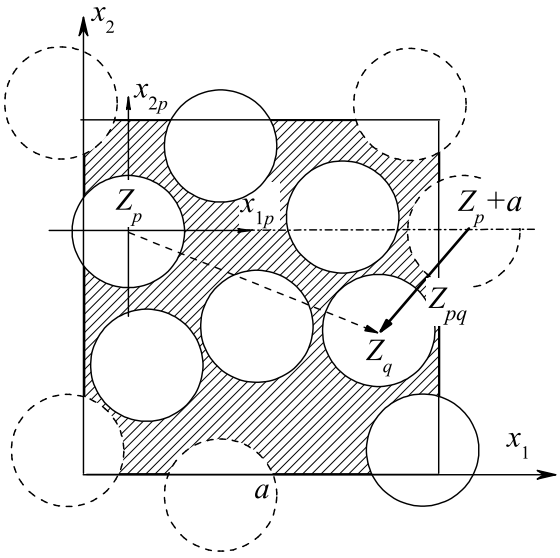

Fig. 1. RUC model of fibrous composite

Besides the global Cartesian coordinate system Ox_1x_2, we introduce the local, fiber-related coordinate systems $Ox_{1q}x_{2q}$ with origins in O_q. Also, we will use the following complex-value variables

$$z = x_1 + \mathrm{i}x_2, \qquad z_q = x_{1q} + \mathrm{i}x_{2q}; \tag{5}$$

representing the point $x = (x_1,\, x_2)^T$ in the complex planes Ox_1x_2 and $Ox_{1q}x_{2q}$, respectively. The global complex variable $z = z_q + Z_q$, where $Z_q = X_{1q} + iX_{2q},\ q = 1, 2, \ldots, N_p$. The local, fiber-associated variables $z_p = z - Z_p$ relate each other by $z_q = z_p - Z_{pq}$, where $Z_{pq} = Z_q - Z_p = X_{1pq} + iX_{2pq}$ is the complex number defining relative position of the fibers with indices p and q. The parameter Z_{pq} is understood here as the minimum distance between the fibers of pth and qth lattice type arrays (solid arrow in Fig. 1) and implies $|X_{jpq}| < a/2,\ j = 1, 2$. In these notations, the fiber-fiber non-overlapping condition is written as $|Z_{pq}| > 2R$. The parameter often introduced in the many-fiber models of FRC is the "minimum allowable inter-fiber spacing" $\delta_{\min} = \min\limits_{p,q} |Z_{pq}|\,/2R - 1$ (Chen and Papathanasiou, 2004). It is usually assigned some small positive value in order to separate inclusions and thus alleviate an analysis (either analytical or numerical) of the model BVP. In our numerical study, we put $\delta_{\min} = 0.01$.

The quasi-random geometry shown in Fig.1 is generated using the molecular dynamics algorithm of growing particles (e.g., Kushch et al., 2008). This model was studied by several authors under assumption that the matrix and fibers are perfectly bonded along the interfaces $L_q, q = 1, 2, \ldots, N_p$.. We consider more general case by assuming the part $L_c^{(q)}$ of interface L_q defined by the endpoints $z_j^{(q)} = \exp(i\theta_j^{(q)})$ $(j = 1, 2)$ separated and the part

$L_b^{(q)} = L_q \backslash L_c^{(q)}$ being perfectly bonded. $\zeta_q = z_q / z_c^{(q)}$, where $z_c^{(q)} = \exp(i\theta_c^{(q)})$ is the crack midpoint: $\theta_c^{(q)} = (\theta_1^{(q)} + \theta_2^{(q)})/2$. $\theta_2^{(q)} - \theta_1^{(q)} = 2\theta_d^{(q)}$; in the prefect bonding case, $\theta_d^{(q)} = 0$. To the best knowledge of the authors, the multiple fiber RUC model with interface cracks never been considered before.

3.2 Problem

By adopting 2D model we assume $\partial \sigma_{ij} / \partial x_3 = 0$: within this framework, the (a) plane strain, (b) plane stress and (c) anti-plane shear (in x_3-direction) problems can be studied. Specifically, we consider the plane strain problem $(u_3 = 0)$. Both the matrix and fiber materials are isotropic and linearly elastic.

The complex displacement $u = u_1 + iu_2$, where u_i are the Cartesian components of displacement vector $u = (u_1,\, u_2)^T$. Specifically, $u = u_0$ in the matrix material with a shear modulus μ_0 and Poisson ratio ν_0 ; u_q, μ_1 and ν_1 refer to displacement and elastic moduli, respectively, of qth fiber, $q = 1,\ 2,\ \ldots,\ N.$. In the adopted by us open-crack model, the traction-free crack surface is assumed. The relevant boundary conditions are:

$$[[u]]_{L_b^{(q)}} = [[T_r]]_{L_b^{(q)}} = 0, \;\; T_r|_{L_c^{(q)}} = 0, \quad q = 1, 2, \ldots, N_p. \tag{6}$$

where $T_r = \sigma_{rr} + i\sigma_{r\theta}$ is the complex traction at the circular interface $L^{(q)}$. Here, $[[f]]_L = f|_{L_+} - f|_{L_-}$ denotes the function f jump through the interface L, L_+ and L_- being the matrix and fiber, respectively, sides of interface L.

We consider the macroscopically uniform stress state of the composite bulk, which implies constancy of the volume-averaged, or macroscopic, strain $\mathbf{E} = \{E_{ij}\} = \{\langle \varepsilon_{ij} \rangle\}$ and stress $\mathbf{S} = \{S_{ij}\} = \{\langle \sigma_{ij} \rangle\}$ tensors, where $\langle f \rangle = V^{-1} \int_V f \; dV$ and $V = a^2$ is the cell volume. In the problem we consider, the far field load is given by the macroscopic strain tensor $\mathbf{E}$. This statement is typical in the homogenization problem where the macroscopic, or effective, moduli are to be determined. On the contrary, using the macroscopic stress tensor $\mathbf{S}$ as the load governing parameter is preferable in the local stress concentration study. For this purpose, the established below simple relationships (27) and (28) can be utilized. Next, it is of common knowledge that, under assumption of uniform macroscopic stress, the periodic geometry results in periodicity of the relevant physical fields. In our case, periodicity of the strain and stress fields

$$\sigma_{ij}\,(z + a) = \sigma_{ij}\,(z + ia) = \sigma_{ij}\,(z) \tag{7}$$

can be alternatively regarded as the cell boundary condition providing continuity of the displacement and stress fields between the adjacent cells.

In (7), σ_{ij} are the components of the stress tensor are given by

$$\frac{\sigma_{ij}}{2\mu} = \varepsilon_{ij} + \delta_{ij} \frac{(3 - \varkappa)}{2(\varkappa - 1)} \theta, \qquad \theta = \varepsilon_{11} + \varepsilon_{22}; \tag{8}$$

and $\varepsilon_{ij} = \frac{1}{2}\left(\frac{\partial u_i}{\partial x_j} + \frac{\partial u_j}{\partial x_i} \right)$ are the components of the strain tensor. Due to (7), the displacement field is the quasi-periodic function of coordinates:

$$u(z + a) - u(z) = (E_{11} + \mathrm{i}E_{12})a; \quad u(z + \mathrm{i}b) - u(z) = (E_{12} + \mathrm{i}E_{22})a. \tag{9}$$

3.3 Solution

We consider the RUC model of FRC (Fig. 1), subjected to the uniform macroscopic strain $\mathbf{E}$. In accordance with the superposition principle, we write a general displacement solution of this problem as a sum of the linear far field u^{∞} determined entirely by the $\mathbf{E}$ tensor and the periodic fluctuation, caused by the inhomogeneities. Namely,

$$u_0(z) = u^{\infty}(z) + \sum_{p=1}^{N_p} z_c^{(p)} u_s^{*(p)}(\zeta_p) \tag{10}$$

where the fiber disturbance terms u_p^{*s} are given by the sums over all the square lattice nodes $k = \{k_1, k_2\}$ $(-\infty < k_1, k_2 < \infty)$:

$$u_s^{*(p)}(\zeta_p) = \sum_{\mathbf{k}} u_s^{(p)} \left(\frac{z_p + W_{\mathbf{k}}}{z_c^{(p)}} \right), \quad W_{\mathbf{k}} = (k_1 + \mathrm{i}k_2)a. \tag{11}$$

It has been shown by Kushch et al. (2010b) that $u_s^{*(p)}$ can be expressed in terms of the periodic complex (harmonic) potentials $S_n^*(z) = \sum_{\mathbf{k}} (z + W_{\mathbf{k}})^{-n}$ and their biharmonic $S_n^{**}(z) = \sum_{\mathbf{k}} |z + W_{\mathbf{k}}|^2 (z + W_{\mathbf{k}})^{-(n+2)}$ counterparts (Movchan et al., 1997). In particular,

$$\varphi_s^{*(p)}(\zeta_p) = \sum_{n=1}^{\infty} a_{-n}^{(p)} \left(z_c^{(p)} \right)^n S_n^*(z_p). \tag{12}$$

The exposed above solving procedure, with two amendments, applies to this problem. First, we require $u_0(z)$ (10) to obey the periodicity conditions (9). This condition gives us the far field $u^{\infty}(z)$ (16) coefficients Γ_1 and Γ_2. By substituting (10) into (9) and taking into consideration $S_n^*(z) = S_n^*(z + a) = S_n^*(z + ia) - \delta_{n1} 2\pi i/a$ and $S_n^{**}(z) = S_n^{**}(z + a) = S_n^{**}(z + ia)$, we find

$$\Gamma_1 = \frac{E_{11} + E_{22}}{2} + \mathrm{Re}\,\Gamma_{\Sigma}; \quad \Gamma_2 = \frac{E_{22} - E_{11}}{2} + iE_{12} + \overline{\Gamma_{\Sigma}}; \tag{13}$$

where

$$\Gamma_{\Sigma} = \frac{\pi}{V} \sum_{p=1}^{N} \left[\varkappa_0 a_{-1}^{(p)} \left(z_c^{(p)} \right)^2 - \overline{a_{-1}^{(p)} \left(z_c^{(p)} \right)^2} + c_1^{(p)} \right]. \tag{14}$$

Second, a set of equations from where the unknown series coefficients can be found is written as

$$I_k^{(q)} = \frac{2\mu_0}{2\pi z_c^{(q)}} \int_0^{2\pi} \left\{ u^{\infty}(z) + \sum_{p \neq q}^{N_p} z_c^{(p)} u_s^{(p)}(\zeta_p) + \sum_{p=1}^{N_p} z_c^{(p)} \sum_{\mathbf{k} \neq \mathbf{0}} u_s^{(p)} \left(\frac{z_p + W_{\mathbf{k}}}{z_c^{(p)}} \right) \right\} t_q^{-k} d\theta_q. \tag{15}$$

The integrals entering (15) can be evaluated either analytically or numerically. The far field $u^{\infty}(z)$ is assumed to be linear function of coordinates, i.e.,

$$u^{\infty}(z) = \Gamma_1 z - \overline{\Gamma_2} \overline{z}. \tag{16}$$

Its analytical integration is elementary and yields

$$I_k^{(q)} = \frac{2\mu_0}{2\pi z_c^{(q)}} \int_0^{2\pi} u^\infty(Z_q + z_c^{(q)} t_q) t_q^{-k} d\theta_q = \begin{cases} -2\mu_0 \overline{\Gamma_2} \left(z_c^{(q)}\right)^{-2}, k = -1; \\ 2\mu_0 u^\infty(Z_q)/z_c^{(q)}, k = 0; \\ 2\mu_0 \Gamma_1, k = 1; \end{cases} \tag{17}$$

and $I_k^{(q)} \equiv 0$ otherwise.

The first sum in (15) contains contributions from the adjacent fibers, where Z_{pq} is understood as the minimum distance ($|X_{jpq}| < a/2,\ j = 1, 2$) between the fibers belonging to the lattices with indices p and q, see Fig. 1. It can be integrated either analytically or numerically. The second sum contains contributions from the "far" fibers. Provided the number N_p of fibers in the cell is sufficiently large, the cell size $a \gg 2R$ and $|Z_{pq}| \gg 2R$ for all fibers contributing to this sum. Therefore, analytical integration is justified here and yields

$$\sum_{p=1}^{N_p} \frac{z_c^{(p)}}{z_c^{(q)}} \sum_{n=1}^{\infty} \left\{ \varkappa_0 A_{nk}^{*pq} a_{-n}^{(p)} + n(\overline{B_{nk}^{*pq}} + \overline{C_{nk}^{*pq}}) \overline{a_{-n}^{(p)}} + \overline{D_{nk}^{*pq}} c_n^{(p)} \right\} \tag{18}$$

In (18), the coefficients A_{nk}^{*pq}, B_{nk}^{*pq}, C_{nk}^{*pq} and D_{nk}^{*pq} are given by the formulas from

$$A_{nk}^{pq} = \begin{cases} (-1)^k \frac{(n+k-1)!}{(n-1)!k!} \left(z_c^{(p)}\right)^n \left(z_c^{(q)}\right)^k \Sigma_{n+k}^{pq*}, \quad k > 0; \\ 0, \quad \text{otherwise}; \end{cases} \tag{19}$$

$$B_{nk}^{pq} = \begin{cases} (-1)^{k+1} \frac{(n-k+2)!}{(n+1)!(1-k)!} \left(z_c^{(p)}\right)^{n+2} \left(z_c^{(q)}\right)^{-k} \Sigma_{n-k+2}^{pq*}, k \le 1; \\ 0, \quad \text{otherwise}; \end{cases} \tag{20}$$

$$C_{nk}^{pq} = \begin{cases} (-1)^k \frac{(n-k)!}{(n-1)!(-k)!} \left(z_c^{(p)}\right)^{n+2} \left(z_c^{(q)}\right)^{-k} \Sigma_{n-k}^{pq**}, k < 0; \\ 0, \quad \text{otherwise}; \end{cases} \tag{21}$$

$$D_{nk}^{pq} = \begin{cases} (-1)^k \frac{(n-k-1)!}{(n-1)!(-k)!} \left(z_c^{(p)}\right)^n \left(z_c^{(q)}\right)^{-k} \Sigma_{n-k}^{pq*}, \quad k < 0; \\ 0, \quad \text{otherwise}. \end{cases} \tag{22}$$

where

$$\Sigma_n^{pq*} = \sum_{\mathbf{k} \neq \mathbf{0}} (Z_{pq} + W_{\mathbf{k}})^{-n}, \quad \Sigma_n^{pq**} = \sum_{\mathbf{k} \neq \mathbf{0}} \frac{|Z_{pq} + W_{\mathbf{k}}|^2}{(Z_{pq} + W_{\mathbf{k}})^{n+2}} \tag{23}$$

are the standard harmonic and biharmonic, respectively, lattice sums.(see, e.g., Movchan et al., 1997; Kushch, 2010). After we have $u^\infty(z)$ determined (13) and $I_k^{(q)}$ expressed in terms of $a_{-n}^{(p)}$ and $c_n^{(p)}$ (18), the problem is effectively reduced to that one considered by Kushch et al. (2010). For the details of derivation, see Kushch et al. (2010b).

3.4 Effective stiffness

The analytical solution obtained in the previous Section provides an accurate and efficient evaluation of the local strain and stress fields in any point of the representative cell of composite

and thus enables a comprehensive parametric study of the stress concentrations, the stress intensity factors and energy release rate at the interface crack tips in FRC depending on volume fraction and arrangement of fibers, loading type and interface damage degree. On the other hand, the strain and stress fields given by this solution can be integrated analytically to get the finite form exact expression of the macroscopic, or effective, stiffness tensor $\mathbf{C}^*$ defined by

$$\langle \sigma_{ij} \rangle = C^*_{ijkl} \langle \varepsilon_{kl} \rangle . \tag{24}$$

In the plane strain problem we consider, the stress field is macroscopically homogeneous and governed by the strain tensor $\mathbf{E} = \{\langle \varepsilon_{kl} \rangle\}$. Hence, the effective transverse elastic moduli $C^*_{1111}, C^*_{1122}, C^*_{2222}$ and C^*_{1212} can be determined from (24) as $C^*_{ijkl} = \langle \sigma_{ij} \rangle = V^{-1} \int_V \sigma_{ij} dV$, where the stress field corresponds to the macroscopic strain $E_{kl} = 1$, $E_{k'l'} = 0$ for $k' \neq k$ and $l' \neq l$.

To simplify the integration procedure, we write the bulk and shear invariants of the strain tensor as

$$\theta = \varepsilon_{11} + \varepsilon_{22} = 2 \operatorname{Re} \frac{\partial u}{\partial z}; \quad \varepsilon_{22} - \varepsilon_{11} + 2\mathrm{i}\varepsilon_{12} = -2\frac{\partial \overline{u}}{\partial z}. \tag{25}$$

Then, we apply the Gauss formula written in complex variables as

$$\int\limits_V \frac{\partial u}{\partial z} dV = \frac{1}{2} \int\limits_L u(n_1 - \mathrm{i}n_2) dL, \tag{26}$$

where L is the boundary of V and $(n_1, n_2)^T$ is the outer normal to L unit vector. Integration procedure is rather straightforward (for details, see Kushch et al., 2010b) and gives the simple exact formulas:

$$\frac{S_{11} + S_{22}}{2} = \frac{2\mu_0 (E_{11} + E_{22})}{(\varkappa_0 - 1)} + \frac{2\pi}{a^2} \frac{(\varkappa_0 + 1)}{(\varkappa_0 - 1)} \sum_{q=1}^{N} \mathsf{c}_1^{(q)}. \tag{27}$$

$$S_{22} - S_{11} - 2\mathrm{i}S_{12} = 2\mu_0 (E_{22} - E_{11} - 2\mathrm{i}E_{12}) + \frac{2\pi}{a^2} (\varkappa_0 + 1) \sum_{q=1}^{N} a_{-1}^{(q)} \left(z_c^{(q)} \right)^2. \tag{28}$$

Together with (24), relations (27) and (28) enable evaluation of the effective transverse elastic moduli $C^*_{1111}, C^*_{1122}, C^*_{2222}$ and C^*_{1212} of unidirectional fibrous composite with interface cracks. To find C^*_{2323} and C^*_{1313}, one has to consider longitudinal shear in fiber axis direction. In mathematical sense, this problem is equivalent to the transverse conductivity (2D Laplace) problem. In application to unidirectional fibrous composite with interface cracks, this problem has been solved recently by Kushch (2010) and we use the obtained there the exact, analogous to (28) formula for C^*_{2323} and C^*_{1313} evaluation.

Remind that our analysis is based on the open crack model (6), adopted in the problem statement. The load-free boundary conditions imposed on the surface of an interface crack lead to a crack-tip oscillating singularity and local overlapping of the surfaces in a vicinity of the crack tip (Toya, 1974). However, Chao and Laws (1992) have shown that under uniaxial loading conditions considering the interface contact results in little difference for the transverse Young's moduli of the composite, see also Yuan et al. (1997). Therefore, we expect (24) to be valid for the predominately tensile loads. The compressive loading leads to the interface cracks closure: this case requires a separate, contact mechanics based consideration.

4 Numerical experiment

4.1 Stiffness reduction vs interface crack density

The single fiber cell cannot be regarded as a reliable model of real-world fibrous composite as far as it assumes the fibers to be periodically arranged and equally debonded. Considered by us the multi-fiber RUC model (Fig.1) is much more realistic and flexible in modeling the micro structure and interface damage of random structure FRC. The experimental observations (e.g., Tsai, 1988; Joffe, 1999) show the one-side interface cracks to be a prevailing form of interface damage in a random composite. Their nucleation and propagation is strongly influenced by the local stress field which, in turn, is affected by the elastic interaction between the fibers. The interface debonding criteria is still a subject under study (e.g., Mantich, 2009): the theoretrical model (Toya, 1974) predicts and the instrumental observations (e.g., Zhang et al., 1997) confirm the fact of unstable growth of newly originated crack along the interface up to $\theta_d \approx \pi/3$; after that, it stops or kinks into the matrix. Hence, an interface damage accumulates mainly by adding new interface cracks of approximately same size rather than by gradual stable growth of the pre-existing cracks. Therefore, the interface crack density d defined as a ratio of the number of interface cracks N_{db} to the overall number N_p of fibers per area unit (or, equivalently, per RUC) seems to be an appropriate measure of interface damage level.

In order to estimate an effect of interface crack density $d = N_{db}/N_p$ on the effective elastic moduli of composite, we consider four test problems for the RUC containing $N_p = 100$ fibers ($c = 0.5$), uniaxially loaded in x_2-direction. For all interface cracks, $\theta_d = \pi/3$. In the first two cases, the fibers were arranged in a (10×10) square order. A random subset of $N_{db}(< N_p)$ fibers with interface crack was defined with aid of the random number generator and the effective transverse elastic moduli C^*_{1122}, C^*_{2222} and C^*_{1212} were calculated for the defined this way geometry of RUC. In the case 1, the cracks were equally positioned and centered in the point $\theta_c = \pi/2$ where the normal interface stress reaches a maximum. In the case 2, the upper ($\theta_c = \pi/2$) and bottom ($\theta_c = -\pi/2$) cracks are equally probable. The similar model suggested by Teng (2007) contains a random subset of fibers with entirely debonded interfaces. The cases 3 and 4 are analogous to cases 1 and 2, respectively, but with random arrangement of fibers within the cell.

All the mentioned models possess a certain degree of randomness. In order to get the statistically meaningful data, a series of computer-aided experiments has been performed for each set of input parameters, with subsequent statistical postprocessing. The ensemble-averaged (over 20 runs) simulation results are shown in Figs. 2 and 3 by the solid and dash-dotted lines.d.

As seen from the plots, the effective elastic moduli are substantially affected by the interface damage parameter, d. At the same time, specific (upper/bottom) location of crack has a minor effect for both regular and random arrangement of fibers. Noteworthy, $C^*_{2222}(d)$ is practically insensitive to the fiber packing type whereas the moduli $C^*_{1122}(d)$ and $C^*_{1212}(d)$ of the random structure composite are considerably higher as compared with the periodic one.

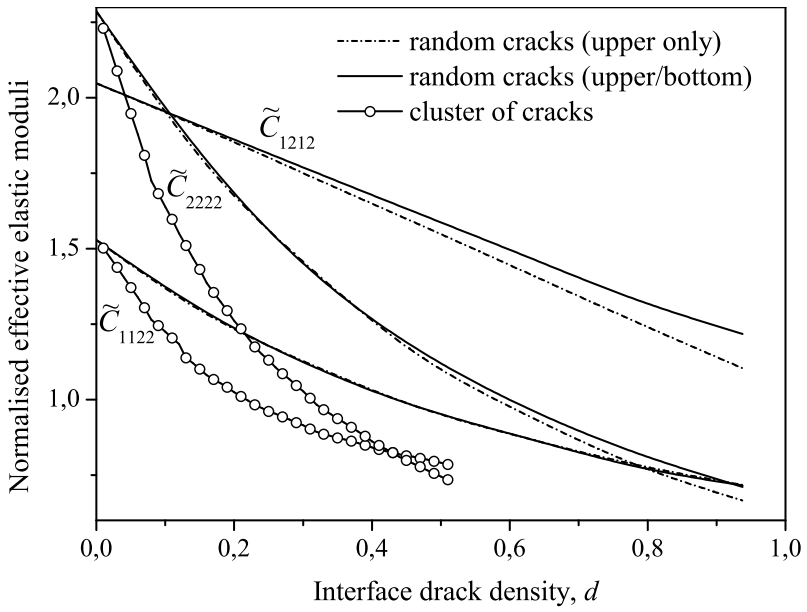

Fig. 2. The effect of interface crack density (periodic composite)

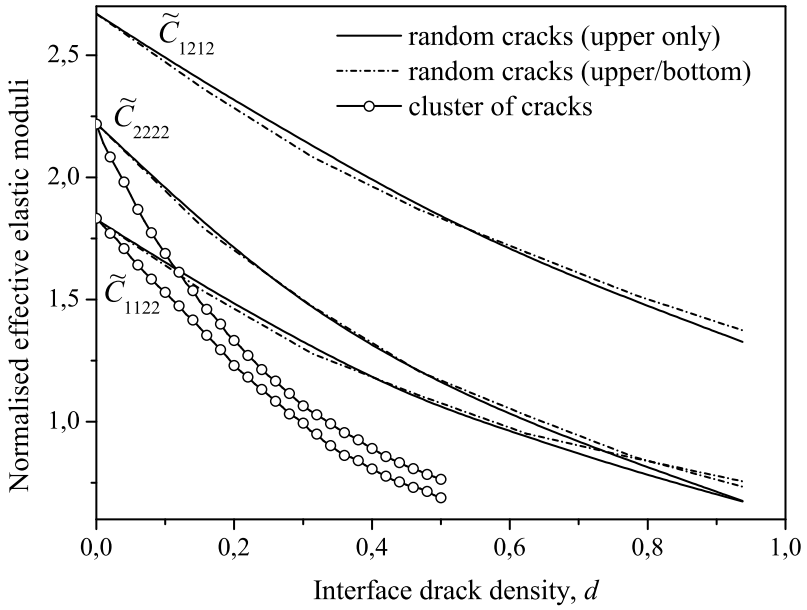

Fig. 3. The effect of interface crack density (random composite)

4.2 Modeling the interface crack cluster formation

The considered above models enable an estimate of composite stiffness reduction vs interface crack density. However, a drawback of these models consists in that position and orientation of the interface cracks was prescribed in random manner, regardless of the micro geometry and local stress field. In fact, micro geometry of fibrous composite and loading type predetermine, to a large extent, the interface damage development. It seems plausible to suggest the peak interface stress point as the most probable place of interface crack onset. The crack propagation along the interface of a given fiber causes partial unloading of this fiber and re-distribution of the released load between the adjacent fibers. In turn, it increases the stress concentration on them and, hence, risk of damage of the neighboring interfaces, etc. This mechanism is responsible for the interface damage spreading and formation of the observed experimentally

(e.g., Tsai, 1988; Joffe, 1999) chain-like clusters of interface cracks.

To model the interface crack cluster formation, the following iterative algorithm will be used. First, the RUC geometry (either random or periodic) with prescribed fiber volume content is generated and the model problem is solved under assumption that all the fibers perfectly bonded with matrix. The uniaxial tensile load is applied in x_2-direction. Next, we evaluate local stress field and look for a point where the absolute maximum of the normal interface stress is reached. Then, we modify the model geometry by adding the interface crack (as before, $\theta_d = \pi/3$) centered in this point and solve the model problem again, etc. The aim of this simulation is to answer the question: how does debonding propagate?

We start with the periodic (10×10) RUC geometry ($N_p = 100$) where, in absence of debonding, all the fibers are equivalent. In order to produce an initial disturbance, a single interface crack with $\theta_c = \pi/2$ is nested in the central part of cell.In Fig. 4, the interface cracks are

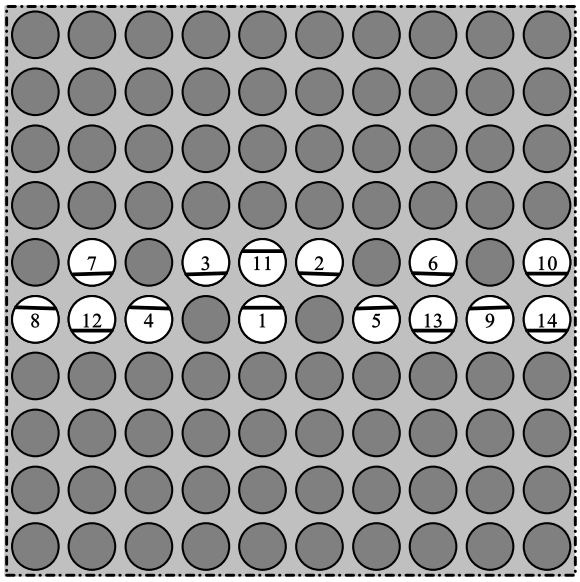

Fig. 4. The interface cracks cluster (periodic composite)

shown by the line segments (chords), the consecutive numbers demonstrate an order in which the cracks appear. As seen from the plot, a chain of interface cracks is orthogonal to the loading direction and grows in two sides simultaneously. An analysis shows that clustering greatly accelerates the effective stiffness loss in the direction of loading. For the periodic composite weakened by the uniformly distributed interface cracks ($d = 0.1$), $\widetilde{C}_{1122} = 1.38$ and $\widetilde{C}_{2222} = 1.97$, see Fig. 3. For the clustered structure with the same cracks density shown in Fig. 4, $\widetilde{C}_{1122} = 1.22$ and $\widetilde{C}_{2222} = 1.64$. For $d = 0.2$, an effect of cluserization is even more pronouncing: $\widetilde{C}_{1122} = 1.23$, $\widetilde{C}_{2222} = 1.68$ and $\widetilde{C}_{1122} = 1.02$, $\widetilde{C}_{2222} = 1.26$ in the case of uniform and clustered distribution of interface cracks, respectively. It is not obvious, however, that this crack density can be reached because, after formation of the chain of interface cracks shown in Fig. 4, the most probable event is their kinking into matrix and coalescence into the macro crack.

The analogous simulations for the random geometry RUC have been performed. The typical

result of simulations is shown in Fig. 5. Here, we also observe a clear tendency of the interface cracks cluster formation, but after a certain period of initial scattered damage accumulation. It has been shown elsewhere (e.g., Kushch et al., 2008) that the random structure composite contains a relatively small fraction of fibers with rather high stress concentration. These fibers debond at the initial stage of loading; then, the chain-like cluster of interface cracks starts to develop. The effective moduli $\widetilde{C}_{1122}$ and $\widetilde{C}_{2222}$ are equal to 1.50 and 1.70, respectively,

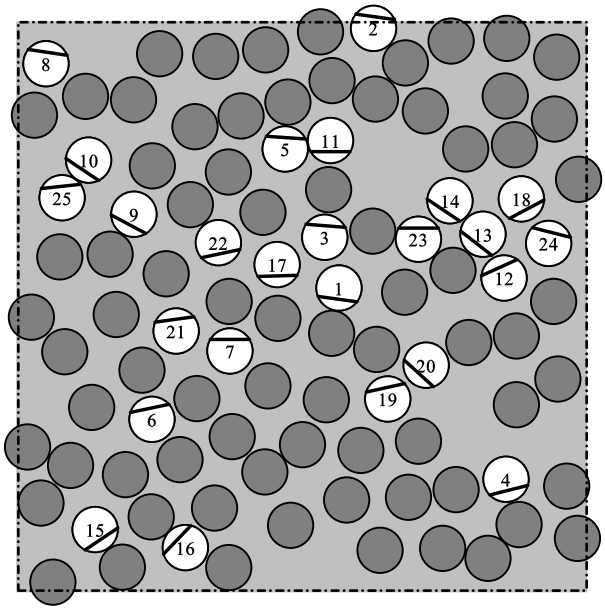

Fig. 5. The interface cracks cluster (random composite)

for $d = 0.1$ and 1.23 and 1.36 for $d = 0.2$. For comparison, the moduli $\widetilde{C}_{1122}$ and $\widetilde{C}_{2222}$ of composite with uniformly distributed cracks (Fig. 6) are equal to 1.65 and 1.96 ($d = 0.1$) and 1.48 and 1.71 ($d = 0.2$). The dependencies $\widetilde{C}_{1122}(d)$ and $\widetilde{C}_{2222}(d)$ in the case of clustered interface cracks are shown by the open circles in Figs 2 and 3 for the regular and random fiber arrangement,respectively. The conclusion drawn from this study consists in that clustering the interface cracks greatly reduces the effective stiffness in the loading direction and increases the damage-induced elastic anisotropy of fibrous composite.

Noteworthy, a similar debonding pattern is observed in the random structure FRC by Kushch et al (2008) who used the RUC model under complete debonding assumption.

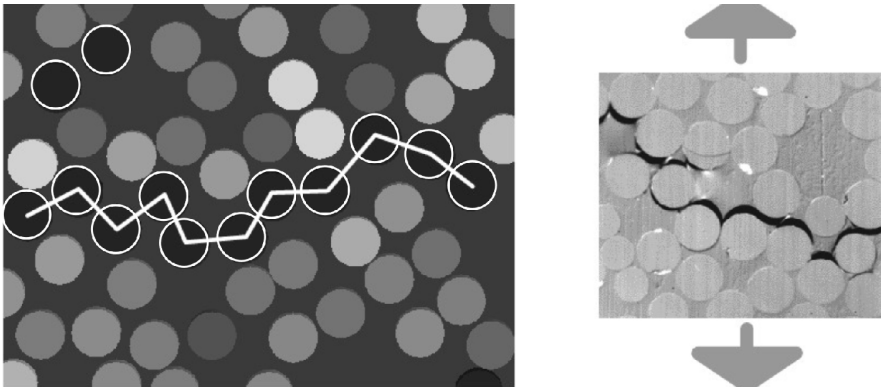

(a) (b)

Fig. 6. Debonding path in the random structure FRC:
(a) - simulation by Kushch et al (2008), (b) - experiment by Gamstedt and Andersen (2001)

In Fig. 6a, the typical simulation result is given whereas Fig. 6b shows the experimentally observed (Gamstedt and Andersen, 2001) crack path. The analogous experimental data have been obtained by other authors (e.g.,Tsai, 1988).

4.3. *Conclusions from numerical study*

Numerical simulation of progressive debonding in fiber reinforced composite using the many-fiber RUC model of composite shows that:

(a) the interface stress grows up rapidly in the area between the fibers perfectly bonded with matrix. In terms of strength, it means that one can expect the interface crack onset at the far load well below the level predicted by the single fiber model;

(b) partial interface debonding causes substantial stress re-distribution and relaxation of the peak interface stress on the neighboring fibers. In terms of strength, it means that the interface crack formation on a given fiber prevents debonding the nearest neighbor fibers. As to the stress relaxation degree, it depends on the crack size and the inter-fiber distance;

(c) the stress intensity factors and the strain energy release rate are greatly contributed from elastic interaction between the fibers and are rather sensitive to the fiber arrangement. In terms of strength, it means that the interface crack propagation is mediated by the neighbor fibers and cracks;

(d) the interface cracks show a clear tendency to form the chain-like clusters, oriented predominantly across the loading direction. Clustering of interface cracks, in turn, accelerates the stiffness loss in the direction of loading and increases the damage-induced elastic anisotropy of the effective elastic moduli of composite.

All said above is especially true for the high-filled FRCs widely used in the engineering practice. It is quite obvious that a single fiber approximation does not work here and one has to look for the multiple fiber models. Among them, the multiple fiber representative unit cell model is, probably, the best choice.

5. Micromechanical theory of FRC damage/strength

Practical significance of the developed approach consists in that it provides the reliable theoretical basis on which the micro mechanics-based theories of FRC strength can be formulated. Below, we consider a simplest theory of this kind which, nevertheless, gives an idea of how available statistical information can be incorporated into the continuum damage model. Specifically, we assume (a) matrix-fiber interface the "weakest link" in FRC and (b) debonding the only micro damage type. Damage criterion is taken in the form $s_m = \max_{\varphi} \sigma_{rr} = \sigma^*$ where the interface strength $\sigma^* = const$ for brittle fracture and $\sigma^* = \sigma^*(N_c) \sim N_c^{-1/m}$ for fatigue, N_c being a number of loading cycles. Alternatively, one can consider σ^* varying randomly from fiber to fiber, with a known statistical rule.

As was said above, at the initial stage of loading, a scattered interface damage is observed at the fibers with a high peak stress and an interaction of defects is relatively weak. This stage is well-described by the statistically substantiated continuum theory of FRC damage/strength, developed by Kushch et al (2009). An elementary damage event is an interface crack onset so it seems natural to consider the interface crack density $d = N_{db}/N_{tot} = \Pr[s_m \ge \sigma^*]$ as a damage parameter. Numerical study shows that there always (regardless of c) exists a relatively low fraction of fibers with high interface stress. The maximum stress is localized between the closely placed fiber pairs and exceeds greatly the mean stress value. In terms of interface strength it means that debonding will occur in these "hot spots" much earlier than in the other sites. This observation correlates well with - and can be quite plausible explanation of - the experimentally observed (Brøndsted et al., 1997; Talreja, 2000; Van Paepegem and Degrieck, 2002; among others) rapid FRC stiffness degradation due to matrix-fiber debonding at the initial stage of cyclic loading. With a high degree of probability, the peak interface stress distribution in FRC with uniform random arrangement of fibers follows Fréchet rule. Using the simulation data, the Fréchet distribution parameters have been found as the functions of fiber volume content c:

$$F_s(\sigma) = \exp\left\{-\left[p_3(c)/\left(\sigma - p_1(c)\right)\right]^{p_2(c)}\right\}. \tag{29}$$

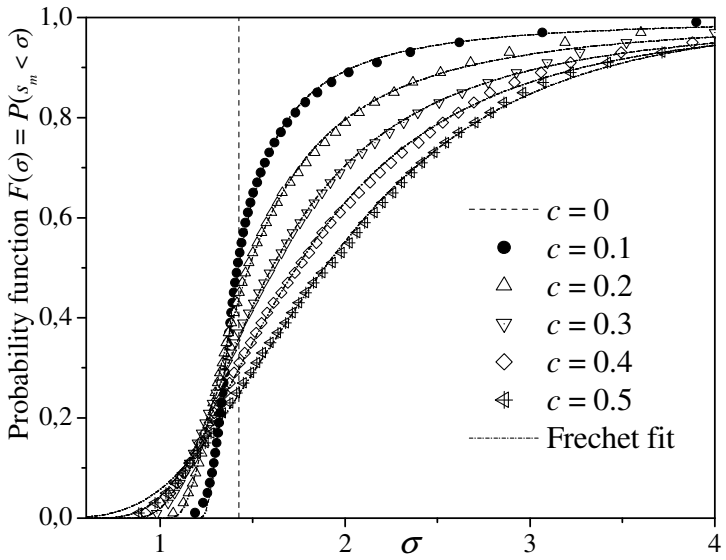

Fig. 7. Empiric probability function of the peak interface stress σ_m: an effect of fiber volume content

Provided N_{tot} taken sufficiently large,

$$d = 1 - \Pr\left[s_m < \sigma^*\right] = 1 - F_s\left(\sigma^* / P\right) \tag{30}$$

This formula estimates the damage level in terms of applied load and interface strength σ^*. Assuming interface degradation due to cyclic loading, one can write the damage accumulation rule in FRC as

$$d(N_c) = 1 - \exp\{-[p_3 / (N_c^{-1/m} / \langle\sigma_{22}\rangle - p_1)]^{p_2}\} \tag{31}$$

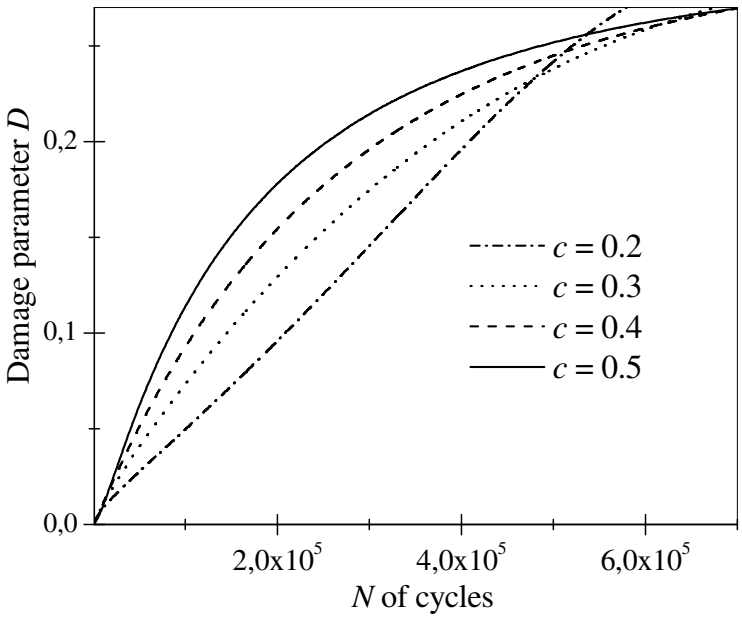

Fig. 8. Interface damage growth of FRC due to cyclic loading

In (30) and (31) we imply d to be low so interactions between the cracks can be neglected. I.e., this model describes an early stage of interface damage development, accompanied by rapid stiffness reduction (e.g., Bronsted et al., 1997; Van Paepegem and Degrieck, 2002). At low d, an effect of interface cracks on the effective elastic modulus of FRC can be approximated by

$$E^*(D) / E^*(0) \approx 1 - \beta D = \beta \exp\{-[p_3 / (N_c^{-1/m} / \langle\sigma_{22}\rangle - p_1)]^{p_2}\} - \beta \tag{32}$$

where β is a factor to be found either experimentally or from simulation (Meraghni et al., 1996; Zhao and Weng, 1997; among others). Together with (31), (32) gives an estimate of stiffness reduction degree vs number of loading cycles. Predicted by our theory normalized effective Young modulus for the fiber volume content c = 0.2, 0.3, 0.4 and 0.5 is shown in Fig. 9, where we put β=1.85 and m=3. As seen from the plot, theory reproduces, at least, qualitatively, the experimental observations by Bronsted et al. (1997) and Van Paepegem and Degrieck (2002). For more details, see Kushch et al (2009).

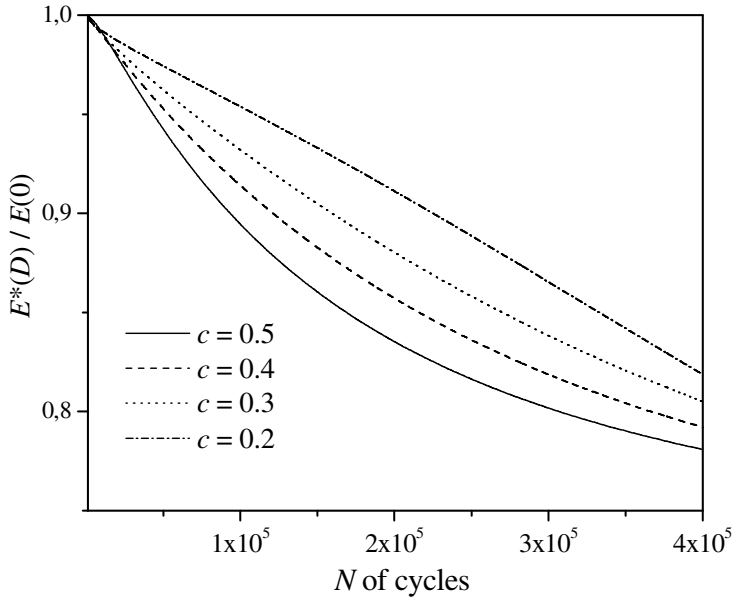

Fig. 9. Stiffness reduction of FRC due to cyclic loading

With the load (and hence damage level) increased, an interaction between the interface defects becomes more and more substantial and leads, in particualr, to the crack clusters formation. It makes practically impossible development of the closed form theory of FRC strength with a scalar damage parameter, able to predict correctly the damage onset and development under the general type loading.

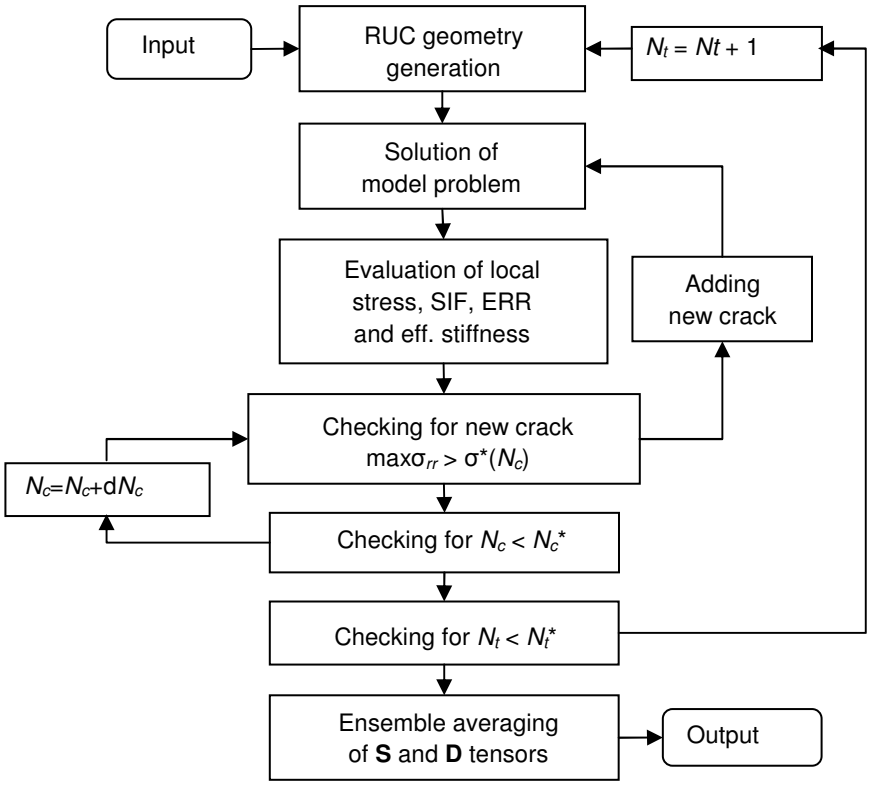

Fig. 10. Flowchart of progressive fatigue damage model

Instead, in a general case:

I. One has to use the tensorial measure of gamage, i.e., the above introduced macro damage tensor **D**.

II. For the micro structure of composite and loading type given, its evolutionary behavior is to be determined from the stepwise computational experiment rather then calculated from the formulas. The typical flowchart of progressive fatigue damage model is shown in Fig.10. Noteworthy, it is similar to those suggested for the continuum (macro level) models of FRC by Shokrieh and Lessard (2000), Tay et al (2008), among others, and consists of the three components: stress analysis, failure analysis, and material property degradation rules.

III. The multi-scale, hierarchical approach is the only way to predict mechanical behavior of FRC correctly. At the macro level, FRC is considered as an anisotropic solid with stiffness **C*** and damage **D** as the internal state variable. The macro stress field of FRC-based structure given by solution of the relevant model problem, defines the loading type assumed in the micro model. Contrariwise, the interface strength value and degradation rate entering the micromechanical model as input parameter, comes from the sub-micro level and hence requires a separate consideration by means of the mechanics and physics of solids. In fact, one has to solve the problem for all three levels simultaneously. This is especially true in the case of fatigue where the history of loading and damage accumulation predetermine the FRC future behavior.

6. Concluding remarks

For each specific composite material, there is a number of factors affecting substantially its strength but not taken into account in our theory. The considered model can readily be generalized in many ways, including (a) loading type, (b) interface debonding criterion, (c) fatigue law, (d) residual (setting) stress, etc. Incorporation of these (as well as other analogous) features makes the model more realistic: at the same time, it necessitates conducting a new series of numerical experiments by analogy with those described above. This work would be the subject of a separate study: here, we emphasize only that the developed approach does not require introducing any simplifying assumptions regarding the stress fields. In contrast to the most existing continuum theories of FRC micro damage (for their comprehensive review see, e.g., Degrieck and Van Paepegem, 2001), we deal with the local, rather than phase-averaged, stress which justifies application of the well-established strength criteria of phase materials and interfaces. Also, the proposed model provides a comprehensive account of microstructure and interactions between the fibers which cannot be expected in the theories based on the mean field or Eshelby-type models. Thus, the proposed approach captures the essential physical nature of the fatigue process and thus provides a reliable theoretical framework for a deeper insight into the fatigue damage initiation and accumulation phenomena in a fiber reinforced composite.

References:

Aghdam, M.M., Falahatgar, S.R., Gorji, M., 2008. Micromechanical consideration of interface damage in fiber reinforced Ti-alloy under various combined loading conditions. Composites Science and Technology 68, 3406--3411.

Benveniste, Y., 1985. The effective mechanical behavior of composite materials with imperfect contact between the constituents. Mechanics of Materials 4, 197-208.

Brøndsted P., Lilholt H., Andersen, S., 1997. Fatigue damage prediction by measurements of the stiffness degradation in the polymer matrix composites. International Conference on Fatigue of Composites Eighth International Spring Meeting, Paris, 3-5 June 1997.

Bystroem, J., 2003. Influence of the inclusions distribution on the effective properties of heterogeneous media. Composites: Part B 34, 587--592.

Caporale, A., Luciano, R., Sacco, E., 2006. Micromechanical analysis of interfacial debonding in unidirectional fiber-reinforced composites. Computers and Structures 84, 2200--2211.

Chao, R., Laws, N., 1992. Closure on an arc crack in an isotropic homogeneous material due to uniaxial loading. Quart. J. Mech. Appl. Math. 5, 629-640.

Chen, X., Papathanasiou, T.D., 2004. Interface stress distributions in transversely loaded continuous fiber composites: parallel computation in multi-fiber RVEs using the boundary element method Composites Science and Technology 64, 1101--1114.

Gamstedt, E.K., Andersen, S.I., 2001. Fatigue Degradation and Failure of Rotating Composite Structures - Materials Characterisation and Underlying Mechanisms. Risø National Laboratory, Roskilde, Denmark.

Ghosh, S., Ling, Y., Majumdar, B., Kim, R., 2000. Interfacial debonding analysis in multiple fiber reinforced composites. Mechanics of Materials 32, 561--591.

Golovchan ,V.T., Guz, A.N., Kohanenko, Yu., Kushch, V.I., 1993. Mechanics of composites (in 12 volumes). Vol.1. Statics of materials. Naukova dumka, Kiev.

Hashin, Z., 1990. Thermoelastic properties of fiber composites with imperfect interface. Mechanics of Materials 8,333-348.

Joffe, R., 1999. Damage accumulation and stiffness degradation in composite laminates. PhD thesis, Lulea University of Technology, Lulea, Sweden.

Ju, J.W., 1991. A micromechanical damage model for uniaxially reinforced composites weakened by interfacial arc microcracks. ASME Journal of Applied Mechanics 58, 923--930.

Kushch, V.I., 2010. Transverse conductivity of unidirectional fibrous composite with interface arc cracks. International Journal of Engineering Science 48, 343--356.

Kushch, V.I., Shmegera, S.V., Mishnaevsky L., 2008. Meso cell model of fiber reinforced composite: Interface stress statistics and debonding paths. International Journal of Solids and Structures 45, 2758-2784

Kushch V.I., Shmegera S.V., Mishnaevsky L. Jr, 2009. Statistics of micro structure, peak stress and interface damage in fiber reinforced composite. *Journal of the Mechanics of Materials and Structures* Vol. 4 (2009), No. 6, 1089–1107

Kushch, V.I., Shmegera, S.V., Mishnaevsky L., 2010. Elastic interaction of partially debonded circular inclusions. I. Theoretical solution. International Journal of Solids and Strucrures 47, 1961--1971

Kushch, V.I., Shmegera, S.V., Mishnaevsky L., 2010b. Elastic interaction of partially debonded circular inclusions. I. Application to fibrous composite. International Journal of Solids and Strucrures (submitted)

Lee, H.K., Simunovic, S., 2001. A damage constitutive model of progressive debonding in aligned discontinuous fiber composites. International Journal of Solids and Strucrures 38, 875--895.

Mantič, V., 2009. Interface crack onset at a circular cylindrical inclusion under a remote transverse tension. Application of a coupled stress and energy criterion. International Journal of Solids and Structures 46, 1287--1304.

Meraghni, F., Blakemad,C.J., Benzeggagh, M.L., 1996. Effect of interfacial decohesion on stiffness reduction in a random discontinuous-fibre composite containing matrix microcracks. Composites Science and Technology 56, 541-555.

Movchan, A.B., Nicorovici, N.A., McPhedran, R.C., 1997. Green's Tensors and Lattice Sums for Elastostatics and Elastodynamics. Proceedings of the Royal Society A453, 643-662.

Prasad, P.B.N., Simha, K.R.Y., 2003. Interface crack around circular inclusion: SIF, kinking, debonding energetics. Engineering Fracture Mechanics 70, 286-307.

Shan, H.-Z., Chou, T.-W., 1995. Transverse elastic moduli of unidirectional fiber composites with fiber/matrix interfacial debonding. Composites Science and Technology 53, 383-391.

Shokrieh, M.M., Lessard, L.B., 2000. Progressive fatigue damage modeling of composite materials. Part I: Modeling. J. Composite Mat. 34 (13), 1056-1080.

Takahashi, K., Chou, T.W., 1988. Transverse elastic moduli of unidirectional fiber composites with interfacial debonding. Metall Trans A 19A, 129--135.

Talreja, R., 2000. Fatigue damage evolution in composites - A new way forward in modeling. In: Proceedings of the Second International Conference on Fatigue of Composites. 4-7 June 2000, Williamsburg.

Tandon, G.P., Pagano, N.J., 1996. Effective thermoelastic moduli of a unidirectional fiber composite containing interfacial arc microcracks. J Appl Mech 63, 210--217.

Tay, T.E., Liu, G., Tan,V.B.C., Sun, X.S., Pham, D.C., 2008. Progressive Failure Analysis of Composites. Journal of Composite Materials 42, 1921

Teng, H., 1992. On stiffness reduction of a fiber-reinforced composite containing interfacial cracks. Mech Mater 13, 175--183.

Teng, H., 2007. Transverse stiffness properties of unidirectional fiber composites containing debonded fibers. Composites: Part A 38, 682--690.

Theotokoglou, E.N., Theotokoglou, E.E., 2002. The interface crack along a circular inclusion interacting with a crack in the infinite matrix. International Journal of Fracture 116, 1-23.

Toya, M., 1974. A crack along interface of a circular inclusion embedded in an infinite solid. Journal of the Mechanics and Physics of Solids 22, 325-348.

Tsai, S.W., 1988. Composites Design, 4th Edition, Think Composites, Dayton, Ohio.

Van Paepegem, W., Degrieck, J., 2002. A new coupled approach of residual stiffness for fatigue of fibre-reinforced composites. International Journal of Fatigue 24, 747-762.

Wriggers, P., Zavarise, G., Zohdi, T.I., 1998. A computational study of interfacial debonding damage in fibrous composite materials. Comput Mater Sci 12, 39--56.

Yeh, J.R., 1992. The effect of interface on the transverse properties of composites. International Journal of Solids and Strucrures 29, 2493--2502

Yuan, F.G., Pagano, N.J., Cai, X., 1997. Elastic moduli of brittle matrix composites with ionterfacial debonding. International Journal of Solids and Strucrures 34, 177-201.

Zhang, H., Ericson, M.L., Varna, J., Berglund, L.A., 1997. Transverse single-fibre test for interfacial debonding in composites: 1. Experimental observations. Composites Part A 28A, 309-315.

Zhao, Y.H. and Weng, G.J., 1997. Transversely isotropic moduli of two partially debonded composites. International Journal of Solids and Structures 34, 493-507.

Zhao, Y.H., Weng, G.J., 2002. The effect of debonding angle on the reduction of effective moduli of particle and fiber-reinforced composites. ASME Journal of Applied Mechanics 69, 292--302.

Zheng, S.F., Denda, M., Weng, G.J., 2000. Interfacial partial debonding and its influence on the elasticity of a two-phase composite. Mechanics of Materials 32, 695--709.